Chemical Science

ROYAL SOCIETY OF CHEMISTRY

EDGE ARTICLE

View Article Online
View Journal | View Issue

Cite this: *Chem. Sci.*, 2023, **14**, 5722

All publication charges for this article have been paid for by the Royal Society of Chemistry

Received 22nd December 2022
Accepted 11th April 2023

DOI: 10.1039/d2sc07006e

rsc.li/chemical-science

A crystalline T-shaped planar group 14 anion†

Xiaona Liu,[a] Yuyang Dai,[a] Manling Bao,[a] Wenjuan Wang,[a] Qianli Li,[c] Chunmeng Liu,[a] Xinping Wang *[b] and Yuanting Su *[ab]

Isolable T-shaped planar pnictogen compounds R_3Pn were reported more than three decades ago and have been attracting burgeoning interest in recent years; T-shaped planar group 14 anions, isoelectronic to R_3Pn, however, are still unknown. Herein, we report the synthesis, full characterization, and reactivity of the first crystalline T-shaped planar group 14 anion **4** bearing a trinitrogen pincer ligand. DFT calculations indicate that the tricoordinate germanium center features both an unoccupied 4p orbital and two lone pairs of electrons. Its electron-rich nature allows for the nucleophilic attack on the methyl iodine giving methyl-substituted complex **5** and facile oxidation of the germanium center by elemental sulfur and selenium to furnish unpresented organic anions bearing terminal Ge=Ch (Ch = S or Se) double bonds.

Introduction

The heavier analogues of carboanions, $[R_3E]^-$ (E = Si, Ge, Sn, Pb) are isoelectronic to the tricoordinate pnictogen compounds R_3Pn (Pn = P, As, Sb, Bi). Both derivatives commonly feature a pyramidal or trigonal planar element center with a lone pair of electrons (Fig. 1a) and thus are widely used as nucleophiles or Lewis bases in organic synthesis and catalysis.[1] Interestingly, in 1984 Arduengo and co-workers reported a novel T-shaped planar phosphorus compound bearing a geometrically constrained electron-rich ONO pincer ligand (Fig. 1b), which can transfer two electrons to the phosphorus center, leading to the unusual 10-electron 3-coordinated P atom (10-P-3) in the oxidation state of +1.[2] Over decades, T-shaped planar group 15 compounds have attracted more and more attention owing to their peculiar electronic structures, fascinating reactivity, and potential applications in stoichiometric and even catalytic small molecule activation.[3,4] Compared with the extensive studies on the geometrically constrained group 15 compounds, group 14 analogues are remarkably less investigated[5,6] and T-shaped planar group 14 anions remain elusive despite initial calculations[7] and great efforts on potential precursors by the groups of Arduengo, Driess, Roesky, Wessemann, and Greb (Fig. 1c).[5] This mainly stems from the deficiency of suitable ligands and synthetic routes.

Recently, we have reported a family of neutral and radical anionic T-shaped planar pnictogen species stabilized by a geometrically constrained and sterically bulky NNN pincer ligand **1** (Scheme 1).[3i] Herein, we present the successful implementation of this strategy into group 14 chemistry with the isolation, characterization, and reactivity of the first crystalline T-shaped planar group 14 anion salt (Fig. 1d).

Results and discussion

Synthesis and characterization of the germanium precursor

Reaction of the triamine **1** with three equivalents of ^{n}BuLi in toluene afforded the dimeric lithium salt **2** (Scheme 1 and Fig. 2a). Treatment of half equivalent of **2** with one equivalent of $GeCl_4$ in diethyl ether resulted in a deep purple solution. After workup, dichloride complex **3** rather than the monochloride compound ^{NNN}**LGeCl** was unexpectedly isolated as a purple powder in 35% yield. It is proposed that the salt elimination between **2** and $GeCl_4$ in 0.5 : 1 ratio initially affords the intermediate ^{NNN}**LGeCl**, which is oxidized by another one equivalent of $GeCl_4$ with formation of **3** and $Cl_3GeGeCl_3$ (Scheme 1). DFT calculations at the (U)B3LYP-D3BJ/6-311G(d) level demonstrated that the oxidation reaction occurs reasonably according to the negative Gibbs free energy change (ΔG) value of −12.39 kcal mol^{-1}. Thus, direct addition of two equivalents of $GeCl_4$ to the diethyl ether solution of **2** was carried out and **3** was isolated in a higher yield (61%). The EPR spectrum of **3** at room temperature displays a broad featureless signal centered at g = 1.9994 (Fig. S24†), supporting its radical character. Calculated spin density of **3** at the UB3LYP-D3BJ/6-311G(d) level mainly resides on the nitrogen atoms and the annulated phenyl rings with a small contribution from the germanium nucleus (Fig. S29†).

[a]College of Chemistry, Chemical Engineering and Materials Science, School of Radiation Medicine and Protection, Soochow University, Suzhou 215123, China. E-mail: ytsu@suda.edu.cn

[b]State Key Laboratory of Coordination Chemistry, School of Chemistry and Chemical Engineering, Nanjing University, Nanjing 210023, China. E-mail: xpwang@nju.edu.cn

[c]School of Chemistry and Chemical Engineering, Liaocheng University, Liaocheng 252059, China

† Electronic supplementary information (ESI) available. CCDC 2121988–2121991, 2201768 and 2201769. For ESI and crystallographic data in CIF or other electronic format see DOI: https://doi.org/10.1039/d2sc07006e

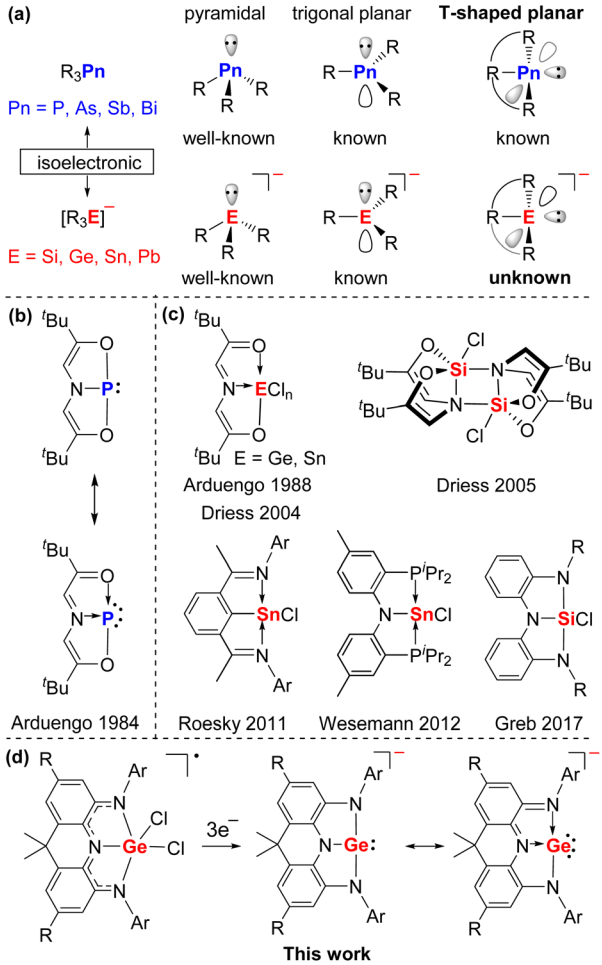

Fig. 1 (a) Molecular shapes of tricoordinate heavier group 14/15 compounds. (b) The first isolable T-shaped planar phosphorus compound. (c) Geometrically constrained group 14 precursors. (d) Present work.

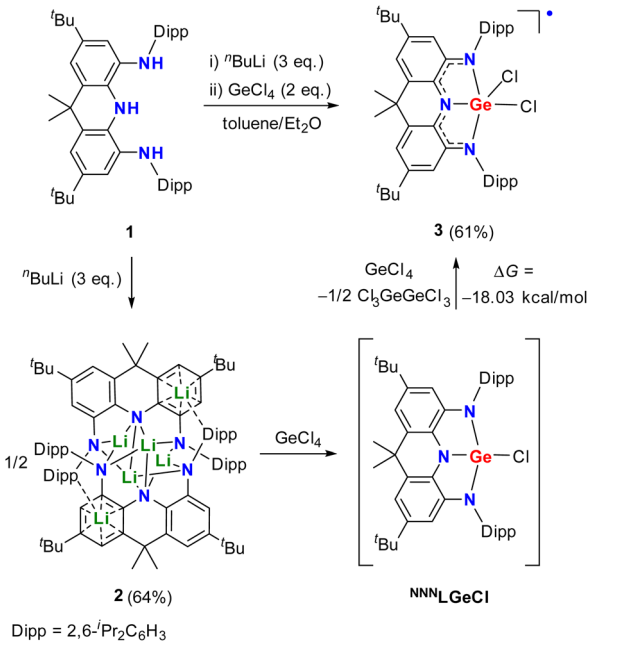

Scheme 1 Synthesis of the germanium precursor **3**.

Crystals of **3** suitable for X-ray crystallographic studies were obtained from its saturated hexane solution. The molecular structure of **3** reveals a square pyramidal coordination of Ge1 by the basal N1, N2, N3, Cl2 atoms and the axial Cl2 atom (Fig. 2b). The Ge1–Cl1 bond (2.091(2) Å) is comparable to the Ge1–Cl2 bond (2.163(2) Å), while the Ge1–N1 (2.011(2) Å) and Ge1–N2 (2.039(3) Å) bond lengths are significantly longer than the Ge1–N3 bond distance (1.872(2) Å). The C–N (1.349(3)–1.387(3) Å) and C–C bond distances (1.404(3) and 1.402(3) Å) in two C_2N_2Ge rings are comparable to those of transition metal complexes featuring the NNN ligand in a diamido imino form.[8] The UV-vis spectrum of **3** exhibits two absorption bands at 400 and 580 nm, the latter of which is also in the typical range for the dianionic NNN ligand (Fig. S25†).[8]

Synthesis, characterization, and DFT calculations of the T-shaped planar germanium anion salt

With the precursor **3** in hand, we investigated its reduction. Treatment of **3** with five equivalents of potassium graphite in THF under ambient conditions afforded, after work up, triaminogermanate salt **4** as a yellow powder in 58% yield (Scheme 2). The isolated compound **4** is extremely moisture- and oxygen-sensitive but is stable both in solution and in the solid state when stored under an inert atmosphere at room temperature. The ^{1}H and ^{13}C{^{1}H} NMR spectra of **4** in THF-D_8 show only one set of resonances for Dipp (Dipp = 2,6-^{i}Pr$_2$C$_6$H$_3$) substituents and annulated arenes (Fig. S3 and S5†), suggesting the C_{2v} symmetrical structure in solution.

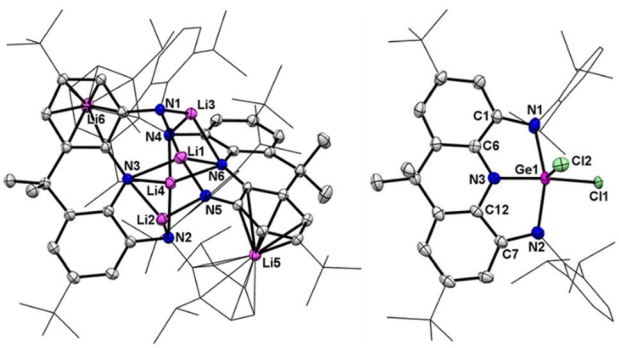

Fig. 2 Left: Solid-state structure of **2**. Right: solid-state structure of **3**. The ^{t}Bu and Dipp groups are simplified as wireframes and hydrogen atoms are omitted for clarity. Thermal ellipsoids are set at the 30% probability level. Selected bond lengths (Å) and angles (°) for **2**: Li1–N1 1.890(4), Li1–N3 2.254(4), Li1–N5 1.903(4), Li1–N6 2.236(4), Li2–N2 2.013(5), Li2–N3 2.133(4), Li2–N5 1.992(4), Li3–N1 1.978(4), Li3–N4 2.000(4), Li3–N6 2.157(4), Li4–N2 2.030(4), Li4–N3 2.092(4), Li4–N4 2.038(4), Li4–N6 2.073(4). Selected bond lengths (Å) and angles (°) for **3**: Ge1–Cl1 2.091(2), Ge1–Cl2 2.163(2), Ge1–N1 2.011(2), Ge1–N2 2.039(2), Ge1–N3 1.872(2), C1–N1 1.387(3), C7–N2 1.379(3), C6–N3 1.349(3), C12–N3 1.362(3), C1–C6 1.404(3), C7–C12 1.402(3), N1–Ge1–N2 153.22(10), N1–Ge1–N3 80.34(8), N2–Ge1–N3 79.59(9), Cl1–Ge1–Cl2 104.09(10).

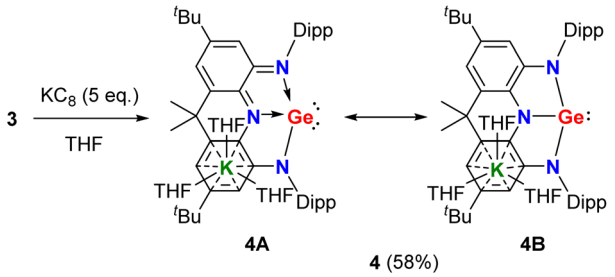

Scheme 2 Synthesis of the T-shaped planar germanium anion salt **4**.

In the solid-state structure of **4**, the solvated counter cation $[K(THF)_3]^+$ interacts with one annulated aryl ring in a η^6 form and the distance between the germanium atom and potassium cation is 5.137 Å, which is larger than a sum of the van der Waals' radii of Ge and K (4.86 Å),[9] suggesting no interaction between them (Fig. 3). The two fused C_2N_2Ge five-membered rings in **4** are almost coplanar with the sum of internal pentagon angles of 540° and 539.97°, respectively. Most strikingly, the germanium center in **4** is only coordinated by three nitrogen atoms to form a T-shaped planar geometry with a large N1–Ge1–N2 bond angle of 153.81(7)°. Upon reduction, the endocyclic N–Ge–N bond angles (78.23(7)° and 76.56(7)°) in **4** become more acute with respect to those (80.34(8)° and 79.59(9)°) of **3**, thus reflecting the elongation of both the equatorial Ge1–N3 bond (1.9039(19) Å) and axial Ge1–N1/N2 bonds (2.0578(18) and 2.1633(18) Å) in **4**. Additionally, the equatorial Ge1–N3 bond distance is shorter than those (1.925(7)–1.970(4) Å) in trinitrogen substituted germanides in pyramidal geometries,[10] and the axial Ge1–N1/N2 bonds are longer, which are in good agreement with the calculated results reported by Arduengo and co-workers.[7] Moreover, it is noteworthy that the average C–N (1.376(3) Å) and C–C (1.421(3) Å) bond distances in two C_2N_2Ge rings are between corresponding single and double bonds, implying that **4** is best viewed as a resonance of canonical forms **4A** and **4B** (Scheme 2), which represents an analogue of T-shaped bismuth(I/III) triamide[3h] and a rare example of valence tautomerism of *p*-block element compounds.[11]

To better understand the electronic structure of the anionic part of **4**, DFT calculations at the B3LYP-D3BJ/6-311G(d) level in consideration of solvent(THF)-correction were carried out. Consistent with the experimental data, the N1–Ge1–N3 and N2–Ge1–N3 bond angles in **4** become narrower and the Ge–N bond lengths are elongated relative to **3**. The natural bond orbital (NBO) analysis reveals that the average Wiberg bond index for the four C–N bonds in **4** is 1.16, demonstrating the partial double bond implied by the form **4A**. Molecular orbital analysis of the anionic part of **4** shows that the lowest unoccupied molecular orbital (LUMO) is mainly the vacant 4p orbital of the Ge atom, while the highest occupied molecular orbital (HOMO) represents a diffuse π-type orbital mainly localized at the Ge center with partial delocalization over the annulated arene rings and nitrogen atoms and the HOMO–2 corresponds to the Ge-centered σ-type lone pair (Fig. 4). Therefore, the tricoordinate germanium center features both an unoccupied 4p orbital and two lone pairs of electrons. Note that the HOMO (−4.11 eV) and HOMO-2 (−4.68 eV) of **4** are comparable to that of the pyrimadal germanium anion $[(NPh_2)_3Ge:]^-$ (−4.32 eV, Fig. S32†) in energy and greatly higher than that of N-heterocyclic germylene $[(DippNCH)_2Ge:]$ (−5.24 eV, Fig. S33†), while the LUMO (−0.63 eV) of **4** is significantly higher than those of its neutral pnictogen analogues ^{NNN}**LE** (E = As: −2.37 eV; E = P: −2.16 eV, Fig. S34 and S35†) and $[(DippNCH)_2Ge:]$ (−1.24 eV), implying its relatively stronger electron-donating and weaker electron-withdrawing ability. The UV-vis spectrum of **4** in THF displays an absorption band at 396 nm (Fig. S26†), which is assigned to HOMO-1 → LUMO and HOMO → LUMO transitions according to the time-dependent DFT calculations (Table S2†).

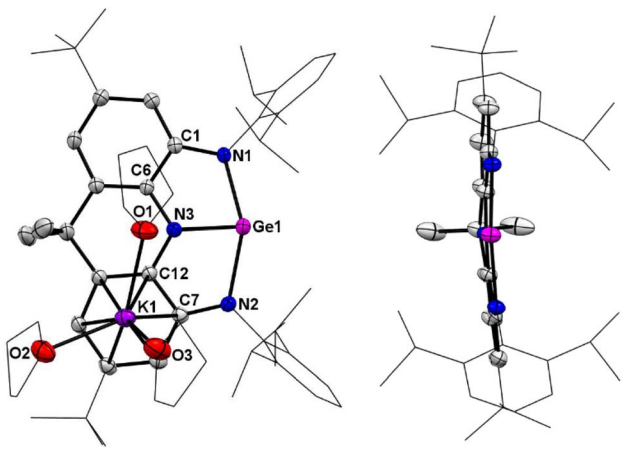

Fig. 3 Left: Solid-state structure of **4**. Right: Side view of the anionic part of **4**. The ^{t}Bu and Dipp groups are simplified as wireframes and hydrogen atoms are omitted for clarity. Thermal ellipsoids are set at the 30% probability level. Selected bond lengths (Å) and angles (°): Ge1–N1 2.0578(18), Ge1–N2 2.1633(18), Ge1–N3 1.9039(19), C1–N1 1.372(3), C7–N2 1.359(3), C6–N3 1.388(3), C12–N3 1.384(3), C1–C6 1.414(3), C7–C12 1.428(3), N1–Ge1–N2 153.81(7), N1–Ge1–N3 78.23(7), N2–Ge1–N3 76.56(7).

Reactivities of the T-shaped planar germanium anion salt

To get insight into the chemical properties of **4**, its reactions were investigated. Treatments of **4** with typical nucleophilic reagents, such as 4-methylpyridine N-oxide, triethylphosphine oxide, KO^{t}Bu and LiMe, were performed at room temperature,

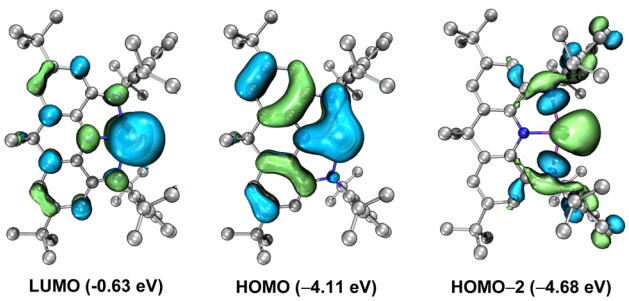

Fig. 4 Key frontier orbitals of the anionic part of **4**. Left: LUMO. Middle: HOMO. Right: HOMO-2.

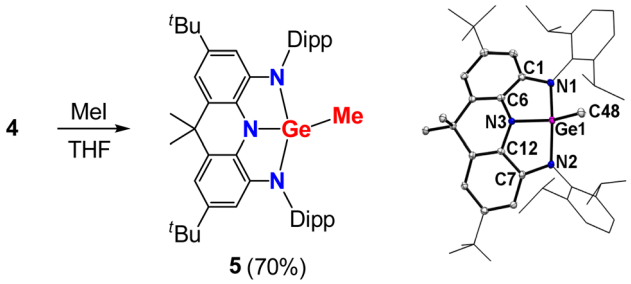

Fig. 5 Left: Reactivity of **4** with methyl iodide. Right: Solid-state structure of **5** (right). The ^{t}Bu and Dipp groups are simplified as wire-frames and hydrogen atoms are omitted for clarity. Thermal ellipsoids are set at the 30% probability level. Selected bond lengths (Å) and angles (°): Ge1–C48 1.9281(18), Ge1–N1 1.8908(15), Ge1–N2 1.8901(15), Ge1–N3 1.8425(14), C1–N1 1.409(2), C7–N2 1.412(2), C6–N3 1.401(2), C12–N3 1.399(2), C1–C6 1.392(2), C7–C12 1.396(2), N1–Ge1–C48 105.00(7), N2–Ge1–C48 104.84(7), N3–Ge1–C48 105.00(7), N1–Ge1–N2 141.84(6), N1–Ge1–N3 86.14(6), N2–Ge1–N3 86.59(6).

and no reaction was observed, supporting its high LUMO in energy. However, reaction of **4** with one equivalent of methyl iodide in THF at room temperature completed within minutes to give compound **5** in 70% yield (Fig. 5). The $^{13}C\{^{1}H\}$ NMR spectrum of **5** displays a typical signal for the terminal methyl at −1.47 ppm (Fig. S10†). Single-crystal diffraction revealed a puckered, bicyclic C_4N_3Ge skeleton with a distorted tetrahedral Ge(IV) center.

Moreover, treatment of a THF solution of **4** with stoichiometric amounts of sulfur at ambient temperature or selenium at 90 °C overnight produced, after removal of the solvent, **6** and **7**, respectively, in moderate yields (Scheme 3). Spectroscopically, the ^{1}H NMR spectra of **6** and **7** exhibit almost identical resonances for only one set of Dipp and annulated arenes (Fig. S13 and S18†), demonstrating their isostructural and symmetrical natures in solution. The ^{77}Se NMR spectrum of **7** displays a singlet at −271.93 ppm (Fig. S23†), which is comparable to those of tetracoordinate germanium(IV) complexes with polar Ge=Se bonds.[12] Structurally, **6** and **7** are also isostructural in the solid-state and exist as a dimer with the anionic units linked by the interactions between the potassium cation and the chalcogenide and aryl groups (Fig. 6). The germanium centers in **6** and **7** are coordinated in a distorted tetrahedral geometry by three nitrogen atoms and one chalcogenide. Upon oxidation,

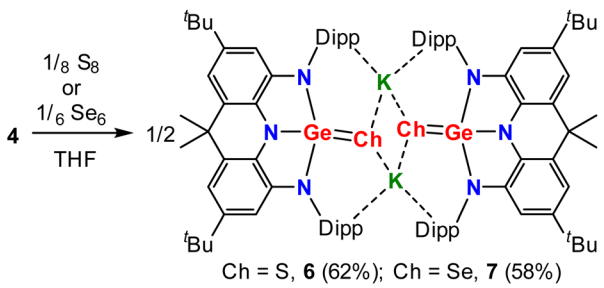

Scheme 3 Reactivity of **4** with elemental chalcogens.

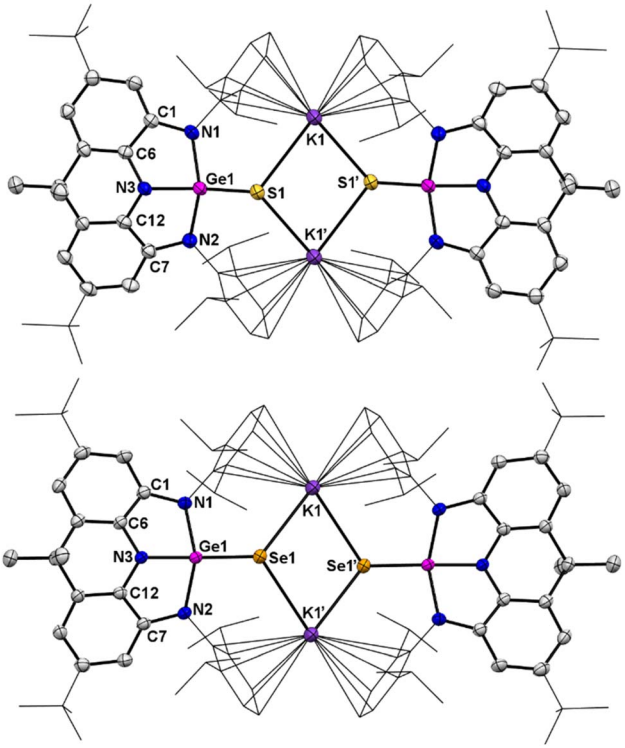

Fig. 6 Top: Solid-state structure of **6**. Bottom: Solid-state structure of **7**. The ^{t}Bu and Dipp groups are simplified as wireframes and hydrogen atoms are omitted for clarity. Thermal ellipsoids are set at the 30% probability level. Selected bond lengths (Å) and angles (°) for 6: Ge1–S1 2.1097(8), Ge1–N1 1.917(3), Ge1–N2 1.916(3), Ge1–N3 1.857(3), K1–S1 3.1094(11), K1–S1′ 3.1491(10), C1–N1 1.394(4), C1–C6 1.394(4), C7–N2 1.396(4), C7–C12 1.395(4), C12–N3 1.403(4), N3–Ge1–S1 142.98(8), N1–Ge1–N2 139.16(11), N1–Ge1–N3 84.41(10), N2–Ge1–N3 84.41(10). Selected bond lengths (Å) and angles (°) for 7: Ge1–Se1 2.2595(12), Ge1–N1 1.928(3), Ge1–N2 1.934(3), Ge1–N3 1.872(3), K1–Se1 3.2541(17), K1–Se1′ 3.2477(17), C1–N1 1.410(4), C1–C6 1.399(4), C7–N2 1.406(4), C6–N3 1.395(3), C12–N3 1.400(3), C7–C12 1.401(4), N3–Ge1–Se1 143.51(8), N1–Ge1–N2 140.30(11), N1–Ge1–N3 84.52(10), N2–Ge1–N3 83.59(10).

all of the Ge–N bond distances in **6** (avg. 1.897 Å) and **7** (avg. 1.911 Å) are contracted relative to those (avg. 1.974 Å) in **3** and are in the normal range for a germanium(IV) complex, while the C–N and C–C bond lengths in fused C_2N_2Ge five-membered rings are slightly elongated and shortened, respectively, and are consistent with the C–N single bonds and aromatic phenyl ring, indicating that the oxidation process occurs at the germanium center accompanied by somewhat intramolecular electron-transfer from the metal centers to the ligands. Notably, the terminal Ge=Ch bonds (Ch = S, 2.1097(8) Å in **6**; Ch = Se, 2.2595(12) Å in **7**) are somewhat longer than those typical Ge=Ch double bonds,[13] but are significantly shorter than the Ge–Ch single bonds (~2.26 Å for Ge–S and ~2.39 Å for Ge–Se bonds)[14] and comparable to the terminal Ge=Ch double bonds (2.12 Å for $[Ge_4S_{10}]^{4-}$ and 2.247–2.287 Å for $[Ge_4Se_{10}]^{4-}$) of inorganic adamantine-like anions $[Ge_4Ch_{10}]^{4-}$,[15] suggesting the existence of polarized (or formal) Ge=Ch double bonds in **6** and **7**. Notably, **6** and **7** represent the first examples of organic anions

bearing terminal Ge=Ch double bonds,[15,16] which are isoelectronic to the well-known R_3Pn=Ch.[17]

Conclusions

More than three decades after the discovery of the T-shaped planar group 15 compound, this work demonstrates that its isoelectronic group 14 anion analog **4** is isolable as well. Compound **4** is prepared from the reduction of the germanium dichloride radical species **3** bearing a trinitrogen pincer ligand. X-ray diffraction studies and DFT calculations reveal that the germanium center in **4** possesses both a vacant 4p orbital and two lone pairs of electrons. The higher HOMO and LUMO of **4** in energy relative to its pnictogen analogues and the N-heterocyclic germylene suggest its relatively stronger nucleophilicity and weaker electrophilicity. Reaction of **4** with MeI gave the methyl-substituted complex **5** and oxidation of **4** with elemental chalcogens readily afforded unpresented organic anions **6** and **7** bearing terminal Ge=Ch (Ch = S or Se) double bonds. Moreover, the trinitrogen pincer ligand exhibits three different oxidation states in the series of germanium complexes: radical anionic form in **3**, diimine amido form in **4**, and triamido form in **5–7**, demonstrating its interesting redox-active properties, which is common for transition metal complexes but is rarely reported for main group elements. Based on these findings, this geometrically constrained non-innocent trinitrogen ligand could be viewed as a potentially suitable building block to stabilize other T-shaped planar group 14 species, which is in progress in our laboratory.

Data availability

Detailed experimental procedures and analytical data are available in the ESI.†

Author contributions

X. Liu performed the major synthesis work and properties study. Y. Dai performed DFT calculations. M. Bao and Y. Dai assisted with the NMR spectra and X-ray single crystallographic diffraction measurements. W. Wang recorded the UV-vis absorption spectra. Q. Li measured the mass spectra. C. Liu acquired some funding. Y. Su and X. Wang conceived the concept and prepared the manuscript. All the authors analysed and interpreted the results.

Conflicts of interest

There are no conflicts to declare.

Acknowledgements

The authors greatly acknowledge financial support from the National Natural Science Foundation of China (Grants 22001184, Y. Su, 22231005, X. Wang, 11904425, C. Liu), the National Key R&D program of China (Grant 2018YFA0306004, X. Wang), the Natural Science Foundation of Jiangsu Province (Grant BK20200849), and the Entrepreneurship and Innovation Talent Program of Jiangsu Province (Y. Su, JSSCBS20210664, C. Liu). We thank the Shanxi Supercomputing Center of China and its Tianhe-2 system for performing calculations.

References

1 Selected references are: (*a*) H.-W. Lerner, *Coord. Chem. Rev.*, 2005, **249**, 781–798; (*b*) V. Y. Lee and A. Sekiguchi, *Acc. Chem. Res.*, 2007, **40**, 410–419; (*c*) V. Y. Lee and A. Sekiguchi, *Organometallic Compounds of Low-Coordinate Si, Ge, Sn and Pb: From Phantom Species to Stable Compounds*, 2010, pp. 89–138; (*d*) C. Prasang and D. Scheschkewitz, *Struct. Bonding*, 2013, **156**, 1–47; (*e*) C. Marschner, *Organosilicon Compounds: Theory and Experiment (Synthesis)*, 2017, vol. 1, pp. 295–360.

2 (*a*) S. A. Culley and A. J. Arduengo, *J. Am. Chem. Soc.*, 1984, **106**, 1164–1165; (*b*) A. J. Arduengo, D. A. Dixon and D. C. Roe, *J. Am. Chem. Soc.*, 1986, **108**, 6821–6823.

3 (*a*) M. Driess, N. Muresan, K. Merz and M. Päch, *Angew. Chem., Int. Ed.*, 2005, **44**, 6734–6737; (*b*) P. Šimon, F. de Proft, R. Jambor, A. Růžička and L. Dostál, *Angew. Chem., Int. Ed.*, 2010, **49**, 5468–5471; (*c*) N. L. Dunn, M. Ha and A. T. Radosevich, *J. Am. Chem. Soc.*, 2012, **134**, 11330–11333; (*d*) S. M. McCarthy, Y.-C. Lin, D. Devarajan, J. W. Chang, H. P. Yennawar, R. M. Rioux, D. H. Ess and A. T. Radosevich, *J. Am. Chem. Soc.*, 2014, **136**, 4640–4650; (*e*) G. Zeng, S. Maeda, T. Taketsugu and S. Sakaki, *Angew. Chem., Int. Ed.*, 2014, **53**, 4633–4637; (*f*) A. Hentschel, A. Brand, P. Wegener and W. Uhl, *Angew. Chem., Int. Ed.*, 2018, **57**, 832–835; (*g*) F. Wang, O. Planas and J. Cornella, *J. Am. Chem. Soc.*, 2019, **141**, 4235–4240; (*h*) M. B. Kindervater, K. M. Marczenko, U. Werner-Zwanziger and S. S. Chitnis, *Angew. Chem., Int. Ed.*, 2019, **58**, 7850–7855; (*i*) M. K. Mondal, L. Zhang, Z. Feng, S. Tang, R. Feng, Y. Zhao, G. Tan, H. Ruan and X. Wang, *Angew. Chem., Int. Ed.*, 2019, **58**, 15829–15833; (*j*) M. Kořenková, M. Hejda, M. Erben, R. Jambor, A. Růžička, E. Rychagova, S. Ketkov and L. Dostál, *Chem. – Eur. J.*, 2019, **25**, 12884–12888.

4 (*a*) A. J. Arduengo and C. A. Stewart, *Chem. Rev.*, 1994, **94**, 1215–1237; (*b*) A. Brand and W. Uhl, *Chem. – Eur. J.*, 2019, **25**, 1391–1404; (*c*) J. Abbenseth and J. M. Goicoechea, *Chem. Sci.*, 2020, **11**, 9728–9740; (*d*) S. Kundu, *Chem. – Asian J.*, 2020, **15**, 3209–3224.

5 For examples of geometrically constrained group 14 compounds, see: (*a*) G. Bettermann and A. J. Arduengo, *J. Am. Chem. Soc.*, 1988, **110**, 877–879; (*b*) M. Driess, N. Dona and K. Merz, *Chem. – Eur. J.*, 2004, **10**, 5971–5976; (*c*) M. Driess, N. Muresan and K. Merz, *Angew. Chem., Int. Ed.*, 2005, **44**, 6738–6741; (*d*) S. Khan, R. Michel, J. R. Dietrich, R. A. Mata, H. W. Roesky, J.-P. Demers, A. Lange and D. Stalke, *J. Am. Chem. Soc.*, 2011, **133**, 17889–17894; (*e*) J. Henning, H. Schubert, K. Eichele, F. Winter, R. Pöttgen, H. A. Mayer and L. Wesemann, *Inorg. Chem.*, 2012, **51**, 5787–5794; (*f*) N. Kramer, C. Jöst, A. Mackenroth and L. Greb, *Chem.–Eur. J.*, 2017, **23**, 17764–17774; (*g*) F. Ebner and L. Greb, *J. Am. Chem. Soc.*, 2018, **140**, 17409–17412; (*h*)

P. Ghana, J. Rump, G. Schnakenburg, M. I. Arz and A. C. Filippou, *J. Am. Chem. Soc.*, 2021, **143**, 420–432; (*i*) F. Ebner and L. Greb, *Chem*, 2021, **7**, 2151–2159; (*j*) H. Ruppert, L. M. Sigmund and L. Greb, *Chem. Commun.*, 2021, **57**, 11751–11763; (*k*) H. Ruppert and L. Greb, *Angew. Chem., Int. Ed.*, 2022, **61**, e202116615.

6 For examples of neutral T-shaped planar group 14 compounds, see: (*a*) J. Flock, A. Sulianovic, A. Torvisco, W. Schoefberger, B. Gerke, R. Pöttgen, R. C. Fischer and M. Flock, *Chem. – Eur. J.*, 2013, **19**, 15504–15517; (*b*) T. Chu, L. Belding, A. Van Der Est, T. Dudding, I. Korobkov and G. I. Nikonov, *Angew. Chem., Int. Ed.*, 2014, **53**, 2711–2715; (*c*) M. T. Nguyen, D. Gusev, A. Dmitrienko, B. M. Gabidullin, D. Spasyuk, M. Pilkington and G. I. Nikonov, *J. Am. Chem. Soc.*, 2020, **142**, 5852–5861.

7 D. A. Dixon, A. J. Arduengo and M. F. Lappert, *Heteroat. Chem.*, 1991, **2**, 541–544.

8 A. I. Nguyen, K. J. Blackmore, S. M. Carter, R. A. Zarkesh and A. F. Heyduk, *J. Am. Chem. Soc.*, 2009, **131**, 3307–3316.

9 M. Mantina, A. C. Chamberlin, R. Valero, C. J. Cramer and D. G. Truhlar, *J. Phys. Chem. A*, 2009, **113**, 5806–5812.

10 (*a*) A. Steiner and D. Stalke, *J. Chem. Soc., Chem. Commun.*, 1993, 1702–1704; (*b*) M. Veith, O. Schütt and V. Huch, *Angew. Chem., Int. Ed.*, 2000, **39**, 601–604; (*c*) L. Witteman, C. B. van Beek, O. N. van veenhuizen, M. Lutz and M.-E. Moret, *Organometallics*, 2019, **38**, 231–239.

11 L. Greb, *Eur. J. Inorg. Chem.*, 2022, e202100871.

12 (*a*) Y. Ding, Q. Ma, H. W. Roesky, I. Usón, M. Noltemeyer and H. Schmidt, *Dalton Trans.*, 2003, 1094–1098; (*b*) S. Nagendran and H. W. Roesky, *Organometallics*, 2008, **27**, 457–492; (*c*) S. Sinhababu, R. K. Siwatch, G. Mukherjee, G. Rajaraman and S. Nagendran, *Inorg. Chem.*, 2012, **51**, 9240–9248.

13 (*a*) N. Tokitoh, T. Matsumoto, K. Manmaru and R. Okazazi, *J. Am. Chem. Soc.*, 1993, **115**, 8855–8856; (*b*) T. Matsumoto, N. Tokitoh and R. Okazazi, *Angew. Chem., Int. Ed.*, 1994, **33**, 2316–2317; (*c*) T. Matsumoto, N. Tokitoh and R. Okazazi, *J. Am. Chem. Soc.*, 1999, **121**, 8811–8824.

14 (*a*) M. C. Kuchta and G. Parkin, *J. Chem. Soc., Chem. Commun.*, 1994, 1351–1352; (*b*) N. Tokitoh, T. Matsumoto and R. Okazazi, *Bull. Chem. Soc. Jpn.*, 1999, **72**, 1665–1684; (*c*) I. Saur, G. Rima, H. Gornitzka, K. Miqueu and J. Barrau, *Organometallics*, 2003, **22**, 1106–1109.

15 (*a*) J. Y. Pivan, O. Achak, M. Louër and D. Louër, *Chem. Mater.*, 1994, **6**, 827–830; (*b*) K.-Y. Wang, S. Zhang, H.-W. Liu, L. Cheng and C. Wang, *Inorg. Chem.*, 2019, **58**, 12832–12842.

16 (*a*) Y. Xiong, S. Yao, S. Inoue, A. Berkefeld and M. Driess, *Chem. Commun.*, 2012, **48**, 12198–12200; (*b*) D. Sarkar, C. Weetman, S. Dutta, E. Schubert, C. Jandl, D. Koley and S. Inoue, *J. Am. Chem. Soc.*, 2020, **142**, 15403–15411.

17 (*a*) G. Hua and J. D. Woollins, *Selenium and Tellurium Chemistry: From Small Molecules to Biomolecules and Material*, 2011, pp. 1–39; (*b*) R. Davies and L. Patel, *Handbook of Chalcogen Chemistry: New Perspectives in Sulfur, Selenium and Tellurium*, 2nd edn, 2013, vol. 1, pp. 238–306.